Известия Гомельского государственного университета
имени Ф. Скорины, № 6 (153), 2025

Физика

УДК 535.21:621.9.048.7:549.211 EDN: QGGGZG

Investigation of laser processing of CVD diamonds using 532 nm wavelength radiation

YU.V. NIKITYUK, E.B. SHERSHNEV, A.S. SOKOLOV, A.N. SERDYUKOV

A study has been conducted on the processing of CVD diamonds subjected to laser radiation at a wavelength of 532 nm. The finite element method was employed to determine the geometric parameters of the craters generated in the diamonds as a result of laser heating for three different processing scenarios: I – laser radiation exposure along the second-order symmetry axis (L_2), II – exposure along the third-order symmetry axis (L_3), and III – exposure along the fourth-order symmetry axis (L_4). A numerical experiment was carried out using laser power density, pulse duration, and laser beam cross-section radius as factors. The calculations were performed for 125 factor combinations as per the numerical experiment design to ascertain the geometric parameters of the laser-induced craters across the three CVD diamond processing scenarios. The finite element calculations derived from the numerical experiment were used to develop neural network models for the laser processing of CVD diamonds. The effective architectures of artificial neural networks for determining the geometric parameters of laser-induced craters were identified using the TensorFlow library. The experimental studies were conducted on the laser processing of CVD diamonds.
Keywords: laser processing, CVD diamonds, ANN, ANSYS.

Выполнено исследование процесса обработки CVD-алмазов при воздействии лазерного излучения с длиной волны 532 нм. Методом конечных элементов определены геометрические параметры лунок, формируемые в алмазах в результате лазерного нагрева, для трех различных вариантов обработки: I – при воздействии лазерного излучения вдоль оси симметрии второго порядка (L_2), II – при воздействии лазерного излучения вдоль оси симметрии третьего порядка (L_3), III – при воздействии лазерного излучения вдоль оси симметрии четвертого порядка (L_4). Проведен численный эксперимент, в котором в качестве факторов были использованы плотность мощности лазерного излучения, длительность импульса, радиус поперечного сечения лазерного пучка. В соответствии с планом численного эксперимента выполнены расчеты для 125 комбинаций факторов с определением геометрических параметров лазерно-индуцированных лунок для трех вариантов обработки CVD-алмазов. Результаты конечно-элементных расчетов, полученные с использованием численного эксперимента, использованы для создания нейросетевых моделей лазерной обработки CVD-алмазов. С использованием библиотеки TensorFlow определены эффективные архитектуры искусственных нейронных сетей для определения геометрических параметров лазерно-индуцированных лунок. Проведены экспериментальные исследования лазерной обработки CVD-алмазов.
Ключевые слова: лазерная обработка, CVD-алмазы, ИНН, ANSYS.

Introduction. The advancement of carbon material synthesis technologies has generated significant interest in exploring the applications of these materials across diverse scientific and technological domains. Among these materials, CVD diamonds are particularly notable. Progress in diamond growth technology using the CVD (chemical vapor deposition) method enables the creation of various electronic devices and instruments. Currently, owing to their high thermal conductivity and transparency over a broad spectral range, CVD diamonds are successfully used as output windows for high-power lasers and sources of terahertz. However, alongside their advantages, CVD diamonds present various limitations that impede their broader application. A notable limitation is their significant hardness and chemical inertness, which poses challenges for processing using conventional technologies. A crucial task is the investigation of efficient technologies for processing CVD diamonds, with laser radiation being one of the most effective tools for this purpose [1]–[3], [4].

The authors have successfully employed finite element modeling and artificial neural networks to calculate temperature fields generated during laser processing of materials, including diamonds. In certain cases, a combination of artificial neural networks and the finite element method has been used to model laser processing processes [5]–[13].

This study presents the findings related to the prediction of parameters for laser-induced craters in CVD diamonds, using a blend of the finite element method and artificial neural networks. The study also presents the results from experimental investigations into the laser processing of CVD diamonds via radiation at a wavelength of 532 nm.

Neural network modeling of CVD diamond laser processing. The data for training and testing the neural networks were derived from finite element calculations of the temperature fields created during the laser processing of diamonds, employing the APDL programming language. A model comprising 61,768 Solid70 elements was developed for the calculations, which were conducted for samples configured as a rectangular parallelepiped with geometric dimensions of 200 × 200 × 300 μm. The properties of the diamond used for modeling were sourced from references [3], [5], [14].

The study employed a simplified scheme of diamond transformations during laser processing, encompassing the subsequent stages: CVD diamond → phase transition → graphite → evaporation. The onset of intense diamond graphitization is presumed to occur at a temperature of 2300 K. The diamond → graphite phase transition was modeled through a cyclic verification of the condition that the temperatures at the nodes of the finite element model reached the corresponding values. Once this condition was met, the relevant model elements were assigned with the thermophysical properties of graphite. During the graphitization of diamond, it is noted that the hexagonal planes of graphite develop parallel to the (111) planes of diamond. The calculation of the crater geometries and temperature fields formed in CVD diamonds due to laser heating was performed for three different scenarios:

I – irradiation along the second-order symmetry axis (L_2),

II – irradiation along the third-order symmetry axis (L_3),

III – irradiation along the fourth-order symmetry axis (L_4).

Table 1 presents the parameters used for the finite element modeling of CVD diamond laser processing.

Table 1 – Parameters of laser impact on a CVD diamond

Parameter	Range of values
Laser radiation power density, P_0, 10^{13} W/m^2	3–3,5
Laser pulse duration, t, 10^{-8} s	3,5–4
Laser beam radius, R, 10^{-5} м	4–6

Figure 1 illustrates an example of the calculated shape of a laser-induced crater created by irradiation along the second-order symmetry axis using the following processing parameters: $P_0 = 3{,}5 \times 10^{13}$ W/m^2, $t = 4 \times 10^{-8}$ s, $R = 5{,}5 \times 10^{-5}$ m.

The calculations were performed for 125 combinations of input parameters, 10 of which were used for testing the neural networks (see Table 2). Table 2 presents the input parameter L, which specifies the order of the symmetry axis of the CVD diamond in relation to the direction of laser irradiation. The output parameters were the width and depth of the laser-induced crater (denoted as Lx and Lz, respectively).

Figure 2 illustrates an evaluation of how the input parameters affect the output parameters. The width of the laser-induced crater is most significantly affected by the laser beam radius and the laser radiation power density, while its depth is substantially influenced by the laser radiation power density and the laser pulse duration.

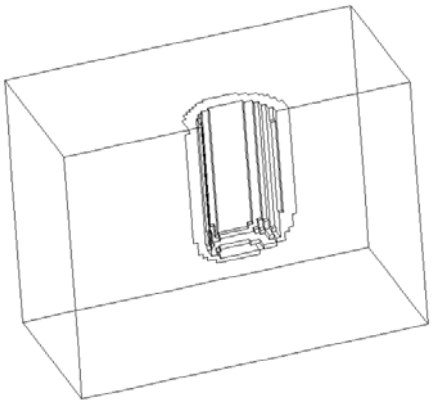

Figure 1 – Calculated crater morphology resulting from laser processing of a CVD diamond

Table 2 – Test dataset

N	P_0, 10^{13} W/m^2	t, 10^{-8} s	R, 10^{-5}m	L	Lx, 10^{-5} m	Lz, 10^{-4} m
1	3,2	3,8	5,0	4	3,5	1,50
2	3,1	3,6	5,0	2	3,0	1,40
3	3,4	3,9	4,5	4	3,5	1,55
4	3,5	3,9	5,0	3	3,5	1,60
5	3,5	3,9	4,0	3	2,5	1,55
6	3,5	3,9	6,0	4	5,0	1,60
7	3,3	3,6	5,5	3	4,0	1,50
8	3,3	3,6	6,0	2	4,5	1,50
9	3,4	3,7	5,0	3	3,5	1,55
10	3,4	3,8	6,0	3	4,5	1,55

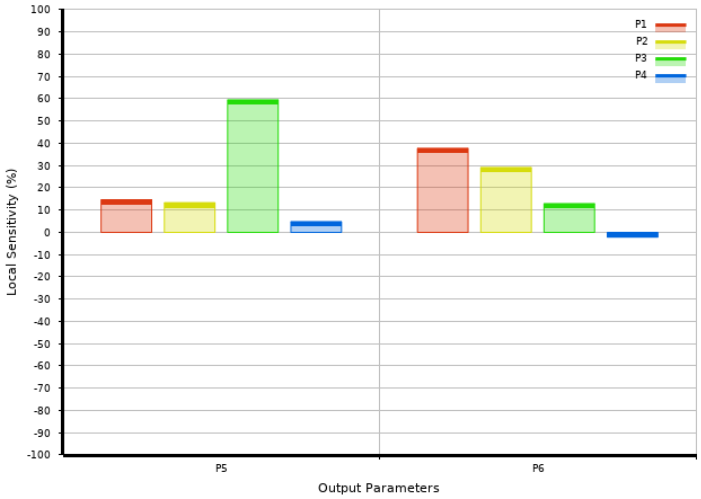

Figure 2 – Sensitivity diagram of the responses: P1 – P_0, P2 – t, P3 – R, P4 – L, P5 – Lx, P6 – Lz

Figures 3 and 4 demonstrate the dependencies of the laser-induced crater parameters on the processing parameters.

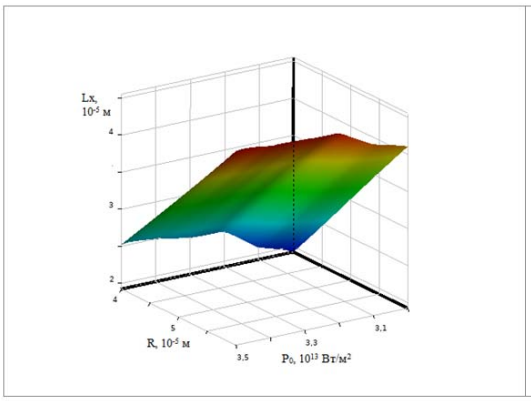

Figure 3 – Dependence of the laser-induced crater width on the processing parameters R and P_0

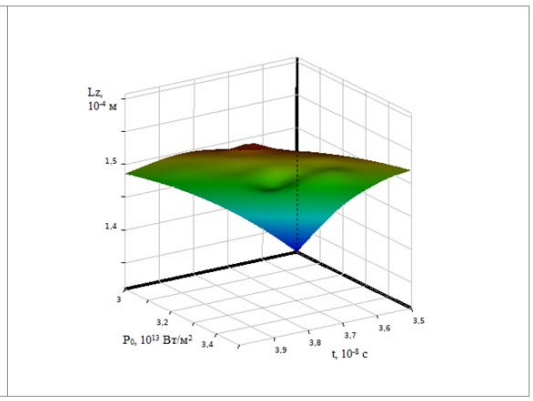

Figure 4 – Dependence of the laser-induced crater depth on the processing parameters P_0 and t

The artificial neural networks with two hidden layers were constructed using the TensorFlow library. The neural networks utilized the Adam optimizer, ReLU activation function, and MSE loss function. The neural networks underwent training for a total of 200 epochs. As a result, 25 neural networks were created with the number of neurons in the two hidden layers ranging from 10 to 50 in steps of 10. The evaluation of the neural network and regression models was performed using the following metrics: Mean Absolute Error (MAE), Root Mean Square Error (RMSE), Mean Absolute Percentage Error (MAPE), and the coefficient of determination R^2.

Figures 5–6 present heat maps showing the distribution of validation errors in determining the geometric parameters of laser-induced craters during laser processing of CVD diamonds. The vertical and horizontal axes represent the number of neurons in the first and second hidden layers of the neural network, respectively. The color coding intensity indicates the magnitude of the error, with a progression from light tones to dark tones indicating an increase in error magnitude.

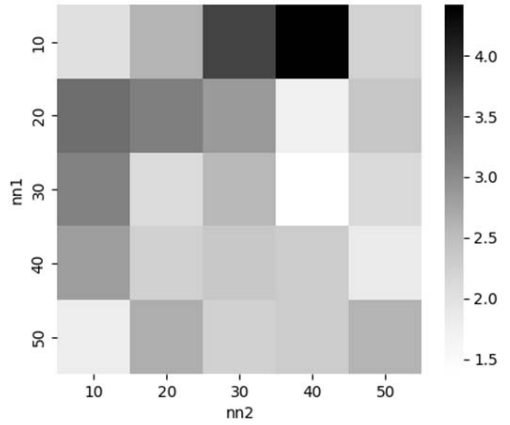

Figure 5 – Heat map of the MAPE error distribution for determining Lx

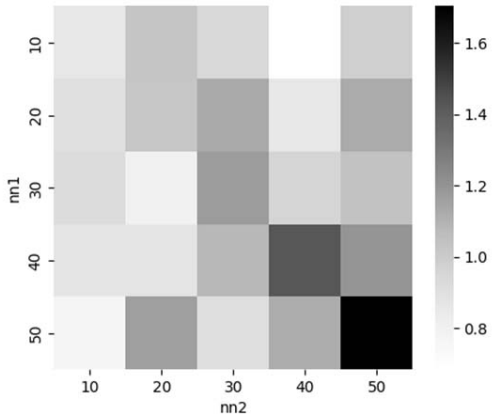

Figure 6 – Heat map of the MAPE error distribution for determining Lz

The neural network with the [4-30-40-2] architecture exhibited the best performance in measuring the width of laser-induced craters, whereas the neural network with the [4-10-40-2] architecture achieved superior results in assessing their depth.

The evaluation results for the corresponding neural network models are detailed in Table 3.

Table 3 – Evaluation results of the neural network models

Criterion	Lx	Lz
RMSE	$6{,}3 \times 10^{-7}$ m	$1{,}5 \times 10^{-6}$ m
MAE	$4{,}8 \times 10^{-7}$ m	$1{,}1 \times 10^{-6}$ m
MAPE	0,96 %	0,68 %
R^2	0,9922	0,9286

The evaluation outcomes of the resulting neural network models lead to the conclusion that the results from neural network modeling must correspond to those of the finite element calculation. This correspondence ensures the possibility of predicting laser processing regimes for diamonds using a combination of the finite element method and artificial neural networks.

Experimental study of CVD diamond laser processing. The experimental work utilized diamonds synthesized by chemical vapor deposition from microwave plasma generated in an acetylene atmosphere at reduced pressure. The discharge was initiated with a microwave generator operating at a frequency of 2,45 GHz. The crystalline structure of the synthesized diamonds was controlled by depositing catalytically active Ir/YSZ layers onto silicon substrates through the magnetron sputtering method [15]–[16].

Figure 7 presents the infrared absorption spectra of the CVD diamonds, obtained via Fourier transform infrared (FTIR) spectroscopy using a Vertex-70 spectrophotometer (Bruker). The presented IR spectra exhibit characteristics typical of CVD diamonds. High transparency is observed in the region of 4000–2700 cm^{-1}, which indicates a low impurity content. The main structure of the spectrum is defined by an intense band in the range of 2700–1700 cm^{-1}, which is the intrinsic diamond lattice absorption band. Below 1700 cm^{-1}, a sharp decrease in absorption intensity is observed. The residual absorption in this region is due to defect-induced processes, which is typical for the polycrystalline structure of CVD diamonds.

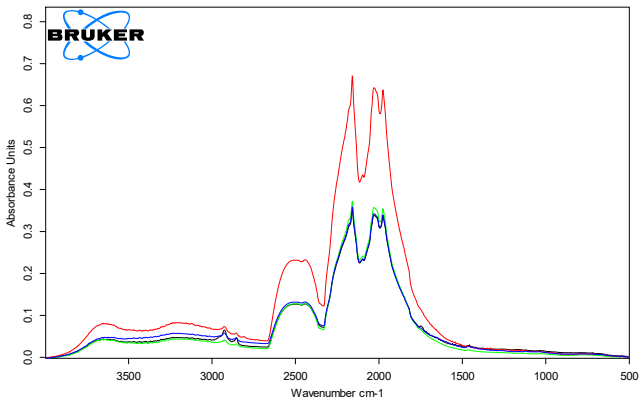

Figure 7 – Absorption spectra of the CVD diamond samples

Figure 8 illustrates the Raman spectra of CVD diamonds obtained using a SENTERRA Raman microscope (Bruker). Spectrum excitation was performed with 532 nm wavelength radiation at a power of 20 mW. The spectra presented show features characteristic of polycrystalline diamonds: an intense diamond peak of about 1330 cm^{-1}; a broad band of about 1480 cm^{-1}; D- and G-peaks at frequencies of 1350 cm^{-1} and 1580 cm^{-1}, which are associated with the graphitic carbon phase.

Experimental investigations into the laser processing of CVD diamonds were conducted utilizing an LS-2134Y YAG:$Nd3^{+}$ laser with electro-optical Q-switching and harmonic generation, which converts 1064 nm radiation to a wavelength of 532 nm. The pulses ranged from one to three in number, with each pulse delivering an energy of 20 mJ.

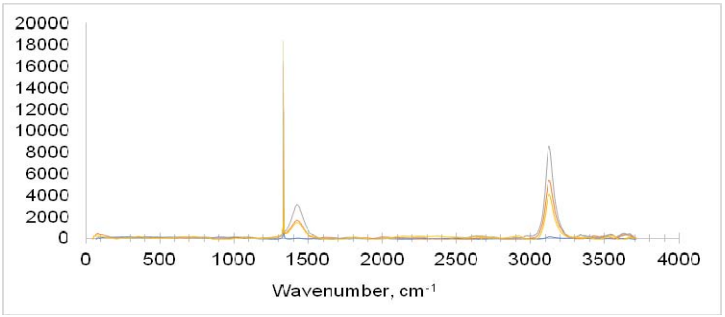

Figure 8 – Raman spectra of the CVD diamond samples

Figure 9 shows the images of the craters formed on the surface of a CVD diamond under exposure to laser radiation with a wavelength of 532 nm and a pulse energy of 20 mJ with different numbers of pulses. The images were obtained using a VEGA II LSH model scanning electron microscope (SEM).

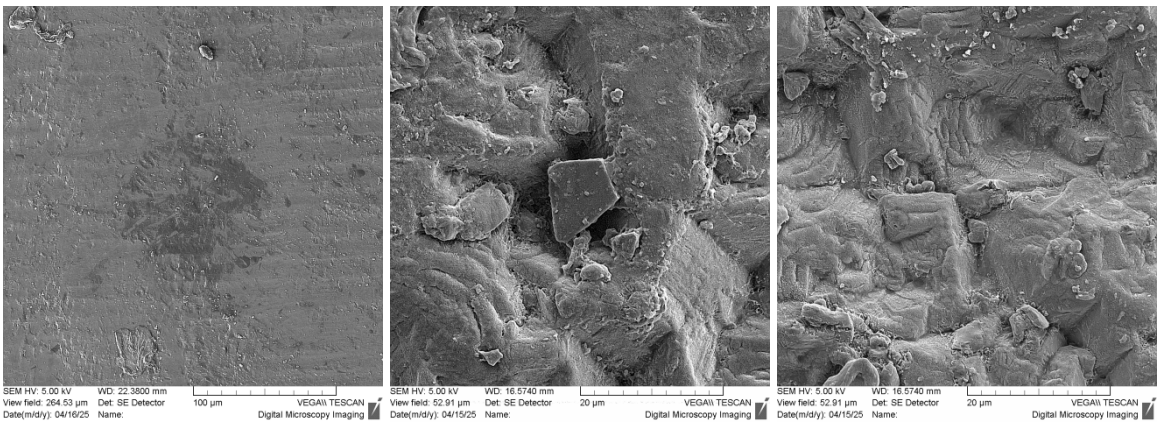

a) b) c)

Figure 9 – Images depicting the surface morphology of laser-induced craters formed in a CVD diamond when subjected to 532 nm wavelength radiation with a pulse energy of 20 mJ for different numbers of pulses: a) 1 pulse; b) 2 pulses; c) 3 pulses

Photograph 9a depicts a crater resulting from a singular pulse. Minimal indentation and minor surface changes are observed, indicating the initial stage of laser exposure. Photograph 9b illustrates a crater following two pulses. A more pronounced indentation and the formation of a thermal affected zone accompanied by microstructural changes are visible. Photograph 9c shows a crater after three pulses. The resulting crater is characterized by the greatest depth and a clearly defined laser ablation zone.

Conclusion. This study performed numerical modeling of the laser processing of CVD diamonds using 532 nm wavelength laser radiation. The finite element method was used to determine the geometric parameters of laser-induced craters under irradiation along different crystallographic symmetry axes. A numerical experiment was performed for 125 combinations of input parameters, such as power density, pulse duration, and laser beam radius, which enabled the generation of a dataset for training and testing artificial neural networks. Neural network models with various architectures were developed and evaluated using the TensorFlow library. The resulting neural network models demonstrated a high degree of agreement with the finite element analysis results, as evidenced by high coefficients of determination and low error levels. Experimental studies were conducted on crater formation on the surface of CVD diamonds when subjected to 532 nm wavelength laser radiation.

Thus, the developed neural network models enable effective prediction of the geometric parameters of craters during laser processing of CVD diamonds, thereby facilitating future optimization of the laser processing parameters for CVD diamonds using 532 nm wavelength radiation.

References

1. Shkadov, A. I. Physical fundamentals of laser processing of diamonds / A. I. Shkadov ; ed. by A. M. Bocharov // Textbook for universities : in 15 books. – Smolensk, 1997. – Book 3. – 288 p.

2. Kononenko, V. V. Laser-stimulated processes on the diamond surface : dis. … doct. physic. and mathematic. science : 01.04.21 / V. V. Kononenko. – Gomel, 2020. – 234 p.

3. Shershnev, E. B. Laser technology for forming components of electronic engineering from amorphous and crystalline materials : author's abstract of Doct. dis. in Techn. Sc. / E. B. Shershnev. – Minsk, 2024. – 48 p.

4. Modeling of graphitization in CVD diamond under the action of laser radiation / D. N. Bukharov, T. A. Khudaiberganov [et al.] // Nanosystems : Physics, Chemistry, Mathematics. – 2025. – Vol. 16, № 4. – P. 427–436.

5. Nikityuk, Yu. V. Laser cleaving of brittle non-metallic materials / Yu. V. Nikityuk, A. A. Sereda, A. N. Serdyukov. – Gomel : Francisk Scorina Gomel State University, 2025. – 218 p.

6. Dependence of the diamond laser processing efficiency on crystallographic directions / S. V. Shalupaev, E. B. Shershnev, Yu. V. Nikitjuk, V. V. Sviridova // SPIE. – 2001. – Vol. 4358. – P. 329–333.

7. Shershnev, E. B. Modeling of laser processing of diamond crystals / E. B. Shershnev, Yu. V. Nikityuk, A. E. Shershnev // Proceedings of F. Skorina Gomel State University. – 2011. – № 6 (69). – P. 164–168.

8. Shershnev, E. B. Features of thermoelastic fields formation during laser processing of diamond crystals / E. B. Shershnev, Yu. V. Nikityuk [et al.]// Problems of Physics, Mathematics and Technics. – 2015. – № 1. – P. 38–40.

9. Shershnev, E. B. Features of using laser radiation with wavelengths of 1064 nm, 532 nm, and 266 nm for processing diamond crystals / E. B. Shershnev, Yu. V. Nikityuk, A. E. Shershnev, S. I. Sokolov // Problems of Physics, Mathematics and Technics. – 2017. – № 1 (30). – P. 22–24.

10. Emelyanov, V. A. Optimization of Laser Processing Parameters for Diamonds / V. A. Emelyanov, E. B. Shershnev [et al.] // Problems of Physics, Mathematics and Technics. – 2022. – № 4 (53). – P. 30–36.

11. Estimating the parameters of laser processing of diamonds using the finite element method and artificial neural networks / V. A. Emelyanov, E. B. Shershnev, Yu. V. Nikitjuk [et al.] // Reports of the Belarusian State University of Informatics and Radioelectronics. – 2023. – Vol. 21, № 4. – P. 40–45.

12. Neural network modeling of laser processing parameters for diamonds in electronics technologies / A. N. Kupo, Yu. V. Nikityuk, E. B. Shershnev, V. A. Emelyanov // Problems of Physics, Mathematics and Technics. – 2025. – № 2 (63). – P. 62–66.

13. Bokiy, G. B. Natural and synthetic diamonds / G. B. Bokiy [et al.]. – M : Nauka, 1986. – 221 p.

14. Novikov, N. V. Physical properties of diamond / N. V. Novikov [et al.]. – M, 1987. – 201 p.

15. Li, J. Preplanting amorphous carbon films based on Ir composite substrates for diamond nucleation / J. Li, B. Zhou, D. G. Piliptsou [et al.] // Journal of Crystal Growth. – 2025. – Vol. 649. – P. 127945.

16. Li, J. Bias-assisted epitaxial Ir/YSZ (1 0 0) substrate for diamond nucleation and growth / J. Li, B. Zhou, Z. Li [et al.] // Journal of Crystal Growth. – 2022. – Vol. 600. – P. 126909.

Гомельский государственный
университет имени Франциска Скорины

Поступила в редакцию 25.09.2025